THE AMERICAN SOCIETY OF MECHANICAL ENGINEERS
345 E. 47th St., New York, N.Y. 10017

96-GT-23

UNBALANCE RESPONSE OF A MULTI-MODE ROTOR SUPPORTED ON SHORT SQUEEZE FILM DAMPERS

R. Youssef and A. El-Shafei
Department of Mechanical Design and Production
Faculty of Engineering
Cairo University
Giza, Egypt

ABSTRACT

This paper describes a fast algorithm to obtain the steady state unbalance response of a multi-mode rotor supported on short squeeze film dampers (SFDs). The presented algorithm is developed based on planar modal theory. Undamped critical speed analysis is first performed to obtain the rotor critical speeds and their associated mode shapes. The modal analysis technique is then applied to the linear part of the rotor-SFD assembly to obtain the system differential equations. The rotor is assumed to execute circular centered orbits, hence all differential equations are reduced to algebraic ones. The resulting equations are manipulated algebraically to form a polynomial in rotor rotational speed. The roots of the polynomial are found and the full unbalance response is obtained. A conventional rotor is used to describe the developed algorithm numerically. Results show that the proposed algorithm gives accurate response in comparison to that obtained by integrating the system differential equations numerically. The great advantage of the proposed algorithm is the saving in the execution time which is extremely dramatic with respect to numerical integration, in addition to other advantages such as the possibility of obtaining all solutions occurring in regions of multiple steady state. Accuracy and speed of execution are quite advantageous regarding parametric studies on multi-mode rotors. These parametric studies can help in the optimization of SFDs design.

NOMENCLATURE

$B = \mu R_j L^3/Mc^3\omega^2_{nl}$ = bearing parameter, nondimensional
c = clearance, m
C_{rr}, C_{tt} = damping coefficients, Ns/m
C^*_{rr}, C^*_{tt} = damping coefficients, nondimensional
d = deflection at disk location, m
$D = d/c$ = deflection at disk location, nondimensional
e = eccentricity, m
F_{rd}, F_{td} = damping forces, N
F^*_{rd}, F^*_{td} = F_{rd}, F_{td} $/Mc\,\omega^2_{nl}$ = damping forces, nondimensional
F_l, F_c, F_r = external complex forces constituting force vector, N
F_{tk} = transmissibility, nondimensional, $k = l$ for left or r for right
$\{f\}$ = n by 1 complex force vector including the external forces, N
$\{f^*\}$ = n by 1 force vector including the external forces, nondimensional
$\{f^*\}_R$ = reduced force vector of size N_f by 1, nondimensional
g = unbalance, m
$g^* = g/c$ = unbalance, nondimensional
$[I]$ = identity matrix
$j = (-1)^{1/2}$
L = journal length, m
m = number of modes
n = number of shaft stations
N_f = number of forces' locations
P = polynomial of order 2m with complex coefficients
P_{real}, $P_{imaginary}$ = real part and imaginary part of P respectively
$\{q\}$ = m by 1 complex vector containing modal displacements, m
$\{\bar{q}\} = \{q\}/c$ = m by 1 complex vector containing modal displacements, nondimensional
$\{\bar{Q}\}$ = m by 1 complex vector containing the modal displacements at the steady state, nondimensional
R = polynomial of order 2m with complex coefficients
R_j = journal radius, m
R_{real}, $R_{imaginary}$ = real part and imaginary part of R respectively
$[U]$ = n by m modal matrix including system eigenvectors
$[U]_R$ = reduced modal matrix of size N_f by m
$\{z\}$ = n by 1 complex vector containing the global displacements
$\{\bar{z}\} = \{z\}/c$ = n by 1 complex vector containing the global displacements, nondimensional

Presented at the International Gas Turbine and Aeroengine Congress & Exhibition
Birmingham, UK — June 10-13, 1996

α, β, δ = phase angles (Figure 3), rad
ε = e/c = eccentricity, nondimensional
μ = fluid viscosity, Ns/m^2
θ = angle (Figure 1), rad
π = 3.141592654....
τ = nondimensional time
ϕ, ψ = angles (Figure 1), rad
ω_{n1} = first natural frequency of the rotor, rad/s
$\{\omega^2\}$ = m by m diagonal matrix containing square of system eigenvalues, rad/s^2
$\{\omega^{*2}\}$ = m by m diagonal matrix containing square of system eigenvalues, nondimensional
Ω = rotor rotational speed, rad/s
Ω^* = Ω/ω_{n1} nondimensional rotor rotational speed
$(\ )^{\cdot}$ = differentiating with respect to time
$(\ )'$ = differentiating with respect to nondimensional time

Subscripts

i = index for mode number
c = denotes rotor midspan
l = denotes left damper
r = denotes right damper

INTRODUCTION

Squeeze film dampers (SFDs) are effective damping devices that are used in gas turbine engines. They proved their ability to attenuate the amplitude of engine vibrations and to decrease the transmitted force to the engine support. Many efforts have been exerted to predict the behavior of SFD supported rotors. Cooper (1963) observed "bistable" operation of a rotor incorporating a SFD, that is the rotor is exhibiting multiple steady state at the same frequency. White (1972) studied theoretically and experimentally the dynamics of a rigid rotor on SFDs. He calculated the forces acting in the damper based on Reynolds equation. He also predicted three steady state orbits of the rotor journal at the same frequency, which agreed with Cooper's work.

Mohan and Hahn (1974) were able to obtain the steady state response of a rigid rotor-SFD system, and they performed parametric studies to determine the effect of the damper's parameters on the rotor behavior. They concluded that, from parametric studies, the SFD is generally an effective damping devise, but for a badly designed damper, the transmitted force can be magnified rather than attenuated.

Taylor and Kumar (1980) did an investigation of the numerical integration techniques used to determine the response of a rigid rotor in SFDs. They were able to demonstrate the drawbacks of numerical integration, and this motivated them (Taylor and Kumar, 1983) to find closed-form steady-state solutions for a rigid rotor in squeeze film dampers by assuming a circular orbit.

Recently, El-Shafei (1990, 1991a) studied the dynamics of a Jeffcott rotor incorporating short and long SFDs. He obtained the steady state unbalance response of the rotor executing circular centered orbit. He considered in his model the effects of fluid inertia.

All the above mentioned analyses are based on single mode rotors. Perhaps the first attempt to obtain the response of multi-mode rotors supported by SFDs, is the work of Greenhill and Nelson (1981) who used an iterative loop using a modified secant method to obtain the response of rotors executing circular centered orbits in SFDs. Later, Mclean and Hahn (1983) developed an algorithm that exploits the characteristics of a circular centered orbit to obtain the response of a multi-mode rotor on SFDs, however their technique needs to be developed mathematically for each particular rotor, and the mathematics can be cumbersome for a complicated rotor. Recently, Bonneau et al. (1989) obtained the dynamical behavior of an elastic rotor with SFD. Also, Hathout et al. (1995) used the modal analysis theory to obtain the transient and steady state response of a multiple mode rotor to control the rotor vibrations by using hybrid squeeze film dampers. They considered the fluid inertia effects in their model.

In this paper, modal analysis theory is exploited, using planar modes, to develop a fast algorithm to obtain the unbalance response of a multi-mode rotor supported on short cavitated squeeze film dampers executing circular centered orbits. A critical speed analysis is first performed to obtain the rotor planar modes, including gyroscopic effects. Planar modes, by definition imply circular orbits (Gunter et al. 1978), which fits well with the assumption of circular centered orbits for the SFDs. In addition, planar modes allow the use of traditional modal analysis rather than the complex modes usually required for modal analysis of rotor systems (Gunter et al., 1978). Through modal analysis and the assumption of circular centered orbits, an extremely fast algorithm is developed to obtain the full unbalance response of multi-mode rotors. The algorithm shows major computer time savings versus numerical integration and also the iterative algorithm developed by Greenhill and Nelson (1981). This allows the current algorithm to be used as a basis for an advanced optimization routine of SFDs, or in its current format can be used for parametric studies of SFD supported rotors.

FORCES IN SFDs

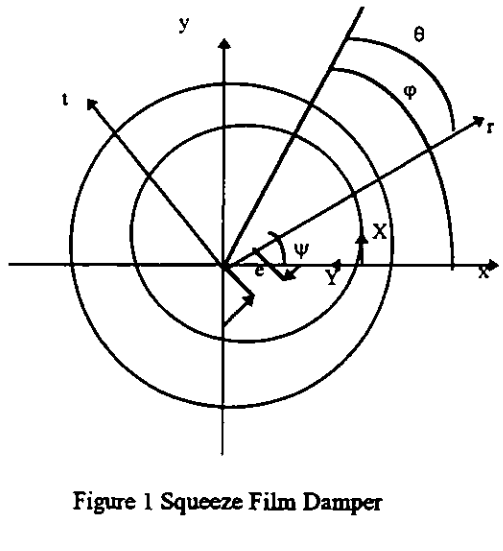

Figure 1 Squeeze Film Damper

Figure 1 shows a side view of the SFD and the coordinate frames used. The forces in the SFD are developed from Reynolds equation (White, 1972).

These damping forces can be derived for a cavitated damper with the journal executing a circular centered whirl for both radial and tangential directions to take the form:

$$F_{dr} = -C_{rt} e\dot{\psi} \tag{1}$$

$$F_{dt} = -C_{tt} e\dot{\psi} \tag{2}$$

where

$$C_{rt} = BC_{rt}^{*}, \qquad C_{tt} = BC_{tt}^{*}$$

where C_{rt}^{*} and C_{tt}^{*} are damping coefficients which are given for the short cavitated damper with a π-film as:

$$C_{rt}^{*} = \frac{2\varepsilon}{(1-\varepsilon^2)^2} \qquad C_{tt}^{*} = \frac{\pi}{2}\frac{1}{(1-\varepsilon^2)^{3/2}}$$

noting that for 2π-film extent C_{rt} becomes zero and C_{tt} is doubled.

As shown above, the forces of SFDs are highly nonlinear in the eccentricity ratio ε, which is the reason for the system nonlinearities.

DEVELOPMENT OF ROTOR-SFDs MODEL USING PLANAR MODAL THEORY

Figure 2 shows a layout of a generic assembly of rotor-SFDs which can be used in various applications. The shaft is supported by two dampers through rolling element bearings at particular locations as shown in the Figure. A set of unbalanced disks are located on the rotor. The dampers and the disks can be located anywhere on the rotor.

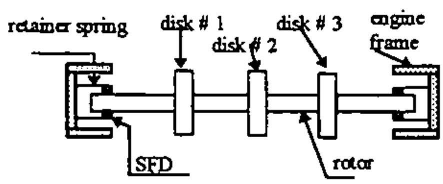

Figure 2 Lay-out of a rotor-SFDs assembly

Implementing the modal analysis technique to such nonlinear rotor-SFDs assembly was developed recently by Hathout et al., (1995). They performed the modal analysis method on the linear part of the rotor and transferred all nonlinear forces to the right hand side as external forces acting on each damper in addition to the unbalance forces acting on the disks.

To apply modal analysis to the assembly shown above, an undamped critical speed analysis is performed on the rotor without including the SFDs taking into consideration the bearing and support stiffness. This analysis is performed on the shaft which is divided into n stations, using available computer programs based either on transfer matrix methods or finite element methods, which include the rotor and disks gyroscopics in the analysis. The analysis would result in m undamped critical speeds of interest with their associated planar modes.

Based on the critical speed analysis and the modal analysis theory (Meirovitch, 1986), and since planar modes are being used, one can obtain the rotor system's differential equations in the modal coordinates as follows (Gunter et al., 1978)

$$\{\ddot{q}\} + [\omega^2]\{q\} = [U]^T\{f\} \tag{3}$$

where $\{q\}$ is an m by 1 vector with complex values ($x+jy$) containing the m modal displacements for the m modes of interest, $[\omega^2]$ is an m by m diagonal matrix with coefficients as the system m natural frequencies squared, $[U]^T$ is an m by n matrix which is the transpose of the modal matrix comprising the m planar mode shapes obtained from the critical speed analysis. Finally, $\{f\}$ is an n by 1 complex vector comprising of non-zero elements only at the stations at which the external forces acting on the system are located. The force vector $\{f\}$ can be defined as

$$\{f\} = \begin{Bmatrix} \text{damping force at the left damper location } (F_l) \\ 0 \\ \vdots \\ 0 \\ \text{unbalance force at the location of disk \# 1 } (F_{u1}) \\ 0 \\ \vdots \\ 0 \\ \text{unbalance force at the location of disk \# 2 } (F_{u2}) \\ 0 \\ \vdots \\ 0 \\ \text{unbalance force at the location of disk \# 3 } (F_{u3}) \\ 0 \\ \vdots \\ 0 \\ \text{damping force at the left damper location } (F_r) \end{Bmatrix}$$

Using the modal transformation, one can obtain

$$\{z\} = [U]\{q\} \tag{4}$$

where $\{z\}$ is an n by 1 vector with complex values comprising the global displacements of the rotor stations.

Equations (3) and (4) can be written in nondimensional form (Hathout, et al., 1995) as

$$\{\bar{q}''\} + [\omega^{*2}]\{\bar{q}\} = [U]^T\{f^*\} \tag{5}$$

$$\{\bar{z}\} = [U]\{\bar{q}\} \tag{6}$$

It should be noticed that the right hand side of equations set (5) would result in an m by 1 vector whose values are only dependent on the elements of the eigenvector corresponding to the stations at which the forces are acting, since the elements of the eigenvectors corresponding to the other stations would be multiplied by the zero values of the force vector $\{f\}$. Thus, it is enough to obtain mode shapes data only at the stations at which dampers and disks are located (i.e. locations which are sources of the external forces). This means that it would be sufficient to use the reduced modal matrix $[U]_R$ which will be reduced to an N_f by m matrix and the force vector $\{f\}$ will be also reduced to an N_f by 1 vector, where N_f is the number of points on the rotor at which the external forces are located.

STEADY STATE ANALYSIS

For the purpose of the following analysis we will assume that only one disk, which is chosen to be the disk # 2, is exhibiting an umbalance. This assumption can be easily removed without affecting the analysis. As a result of this assumption the reduced force vector $\{f^*\}_R$ will be of size N_f=3, due to the forces at the two damper locations and the disk location.

Figure 3 shows a side view of the rotor of Figure 2. Point O represents the center of bearings. Point E_l represents the left journal center, while point E_r represents the right journal center with phase shift α. Thus the distance OE_l is equal to the eccentricity (e_l) of the journal in the left damper, and distance OE_r is the eccentricity (e_r) of the right journal. Point S represents the geometric center of the disk with the umbalance, thus the distance OS is the deflection (d) of the rotor at the disk # 2. Point G represents the center of gravity of the disk, thus the distance SG is the umbalance (g).

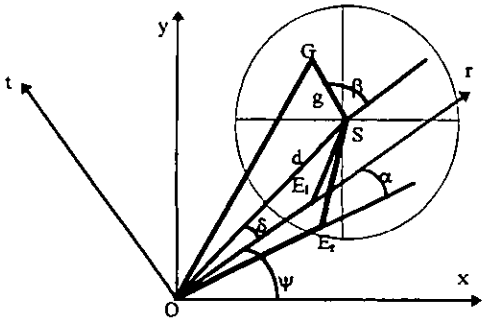

Figure 3 Side view of rotor

Also, shown in Figure 3, the notation and the coordinate frames used in the steady state analysis. The (x,y) frame is a stationary frame whose origin is at the bearing center O. The rotating (r,t) frame which is rotating at the whirl frequency of the system, with its r-axis coinciding with the eccentricity (OE_l) in the left damper. This rotating frame is chosen to be a reference for the eccentricity and forces in the right damper also.

Finally, shown in Figure 3, the general directions of deflections at the specified locations on the rotor (i.e. locations of the acting forces). A phase angle α is considered between the left and right eccentricities. The deflection of the rotor at the disk location (d) makes an angle δ with the positive r-axis (which makes an angle ψ with the positive x-axis). The umbalance (g) is chosen to make a general angle β with the positive r-axis.

DEVELOPMENT OF THE STEADY STATE MODEL

Assuming the rotor is executing a circular centered orbit with synchronous whirl at the speed of the rotor rotational speed Ω^*, and by referring to the system geometry shown in Figure 3, the equation relating the angular speed of the umbalance and the rotor rotational speed Ω^* is given by

$$\psi' = \Omega^* \tag{7}$$

The elements of the vector $\{z\}$ comprising the displacements at the left journal, center of the disk, and the right journal can be assumed to exhibit a circular centered orbit at steady state. Thus the vector $\{z\}$ can be expressed as

$$\{\bar{z}\} = \begin{Bmatrix} \varepsilon_l e^{j\Omega^* \tau} \\ D e^{j(\Omega^* \tau - \delta)} \\ \varepsilon_r e^{j(\Omega^* \tau + \alpha)} \end{Bmatrix} \tag{8}$$

According to equation (7) the umbalance force acting on the disk can be defined in nondimensional form as

$$F_u = g^* \Omega^{*2} e^{j\beta} \tag{9}$$

Thus the reduced force vector $\{f^*\}_R$ can be given in the following complex form as

$$\{f^*\}_R = \begin{Bmatrix} -C_{rl}\varepsilon_l\Omega^* - jC_{tl}\varepsilon_l\Omega^* \\ g^*\Omega^{*2}e^{j\beta} \\ \left(-C_{rr}\varepsilon_r\Omega^* - jC_{tr}\varepsilon_r\Omega^*\right)e^{j\alpha} \end{Bmatrix} \tag{10}$$

The modal displacement vector $\{\bar{q}\}$ can be acting in a general motion, and can be given by

$$\{\bar{q}_i\} = \{\bar{Q}e^{j\Omega^* \tau}\} \tag{11}$$

where $\bar{Q}$ is a complex value and i can take the values 1 to m.

By substituting equation (11) into equation (5), all derivatives will be terminated. Hence, one can obtain a set of algebraic, time invariant, equations representing the modal displacement in the steady state as follows

$$\left[\left[\omega^{*2}\right] - [I]\Omega^{*2}\right]\{\bar{Q}\} = [U]_R^T\{f^*\}_R \tag{12}$$

Also, substituting for $\{\bar{z}\}$ from equation (8) and for $\{\bar{q}\}$ from equation (11) into equation (6), one can get

$$\begin{Bmatrix} \varepsilon_i \\ De^{i\theta} \\ \varepsilon_r e^{i\alpha} \end{Bmatrix} = [U]_s \{\overline{Q}\} \tag{13}$$

The equations set (12) constitute m complex algebraic, nonlinear, equations, i.e. $2m$ real algebraic equations, and equations set (13) constitute 6 ($2N_j$) real algebraic equations. The two sets can be solved numerically by several numerical methods such as Newton-Raphson method or so. But due to their nonlinearities, this way will lead to a tedious trial and error in addition to false convergence in the regions of multiple solutions (Taylor and Kumar, 1980).

Further algebraic manipulations on the two sets of equations (12) and (13) are performed with the purpose of obtaining a polynomial in Ω^* whose coefficients are function in the source of the nonlinearities (ε_l, ε_r). El-Shafei (1990, 1991) was successful to do so for a Jeffcott rotor, exhibiting a single mode, to obtain the full unbalance response directly . In doing so, one should firstly eliminate the phase angles α and β that appear in the equations set (12) enclosed in the force vector (10). To eliminate the phase angle α, it is chosen to substitute for it from the third row of equations set (13) into equation (10). As a result of this substitution, a new set of m complex equations coupled in $\{\overline{Q}\}$ is obtained which are manually manipulated since it is necessary to obtain the elements of the vector $\{\overline{Q}\}$ individually. Consequently, the vector $\{\overline{Q}\}$ is substituted into equations set (13) and by considering the first row, the following equation can be obtained

$$Re^{i\beta} = P \tag{14}$$

where P and R are polynomials in Ω^*, of order $2m$ each, with complex coefficients which are functions in ε_l and ε_r. To eliminate the angle β, equation (14) is divided into two real equations as follows

$$\begin{bmatrix} R_{real} & -R_{imaginary} \\ R_{imaginary} & R_{real} \end{bmatrix} \begin{Bmatrix} \cos\beta \\ \sin\beta \end{Bmatrix} = \begin{Bmatrix} P_{real} \\ P_{imaginary} \end{Bmatrix} \tag{15}$$

which can be solved using Cramer's rule to give

$$\cos\beta = \frac{P_{real} R_{real} - P_{imaginary} R_{imaginary}}{R_{real}^2 + R_{imaginary}^2} \tag{16}$$

$$\sin\beta = \frac{R_{real} P_{imaginary} + R_{imaginary} P_{real}}{R_{real}^2 + R_{imaginary}^2} \tag{17}$$

Finally, by adding the square of equation (16) to the square of equation (17) we can eliminate the angle β and hence we can obtain the desired polynomial of order 8m with real coefficients function in ε_l and ε_r. The roots of this polynomial can be obtained by using an IMSL subroutine such as DZPLRC or DZPORC. We chose the subroutine DZPORC because it is usually more stable and faster. Also, this polynomial can be transferred, using the state-space theory (Friedland, 1986), into a matrix whose eigenvalues are the roots of the polynomial. To do so, the IMSL subroutine DEVLRG is used to obtain the matrix eigenvalues.

All the above steps are organized in an algorithm to be executed by a digital computer. The algorithm is written in a FORTRAN code, and it has the facility to constitute the coefficients of the desired polynomial (as shown above) for m modes.

It should be emphasized that the developed algorithm would permit any changes in the rotor configurations such as changing the dampers position or shifting the disk location, as well as adding more disks to the rotor.

To conduct the previous steps numerically, a conventional rotor is considered and it is required to predict its behavior when supported by a short squeeze film damper. Table 1 shows the operating conditions and the dimensions of rotor-disk-SFDs assembly used for the numerical analysis. First a critical speed analysis was performed on the rotor using the available program CRITSPD, which resulted in five undamped critical speeds, namely at 30 Hz, 68 Hz, 136 Hz, 348 Hz, and 370 Hz. Figure 4 shows the rotor used in the numerical analysis and its five mode shapes.

Table 1 The specifications of the rotor-disk-SFDs assembly.

SFDs Specifications		Rotor-Disk Specifications	
Journal length (L)	25 mm	rotor length	1000 mm
journal radius (R_j)	37.5 mm	rotor total weight	11.57 Kg
fluid viscosity (μ)	0.014 Ns/m^2	disk weight	6.12 Kg
fluid density (ρ)	917 Kg/m^3 at 70° C	rotor diameter	25.4 mm
bearing parameter (B)	0.125	disk thickness	58.0 mm
journal radial clearance (c)	0.75 (mm)	support stiffness	2452 N/mm

By assuming values for both eccentricities (ε_l and ε_r) to be equal (since our rotor is symmetric), the polynomial coefficients can be calculated by the computer code. For other general rotors, an iteration loop has to be included. The roots of the polynomial can then be obtained by calling the IMSL subroutine, and these roots represent the rotor speed Ω^* at steady state. Complex roots are ignored since they do not represent a steady state. Since the rotor can rotate either clockwise or counterclockwise, the routine obtains both positive and negative roots. The negative roots are neglected and the positive roots are retained. By repeating these steps to cover the range of the eccentricity ratio (0 to 1), one can obtain the full unbalance response for such a rotor-SFDs system.

Knowing ε_l, ε_r, and Ω^*, it is possible to obtain the vector $\{\overline{Q}\}$ by substitution in equation set (12), after terminating α. Hence, one can get the deflection of any point on the rotor, for example we can obtain the response at the unbalanced disk location D by direct substitution for $\{\overline{Q}\}$ in the second row of the equation set (13). To confirm the program output, we can calculate ε_r, by direct substitution for $\{\overline{Q}\}$ in the third row of the equation set (13). This is an additional check to assure that the program has converged to the correct roots.

Also, it is possible to calculate the transmissibility F_t to the support, which is defined as the ratio of the magnitude of the force acting in the damper (left or right) to the magnitude of the unbalance force acting on the center disk. Thus the transmissibility is given by

$$F_a = \frac{|F_k|}{|F_u|} \tag{18}$$

where k can take the subscript l for the left damper or r for the right one.

The above technique is performed using a program MULMOD. The program obtains the unbalance response for both a cavitated model (π-film) and an uncavitated model (2π-film). The execution time of the program is approximately 13 minutes regardless of the model used on an IBM 486 DX2-66 personal computer.

ALGORITHM VERIFICATION

To verify the technique described in previous sections, equations sets (5) and (6) are solved by numerical integration using Runge-Kutta 4 method by a program written to obtain the transient response for both models indicated above. The program is run, at a given rotor speed Ω^*, until a steady state is reached. This process is repeated at each speed until covering the required speed range. To do so, we need approximately 6 hours for the uncavitated model and about 20 hours for the cavitated model on the same computer. A comparison between this response and that obtained by the algorithm, described in the previous section, is shown to indicate the robustness of the proposed technique. This comparison is investigated for each model individually, with nondimensional imbalance value g^* equal to 0.1, as shown in Figures 5 and 6. Each Figure is divided into two groups, group (a) for the response obtained by the suggested technique, while group (b) is for that obtained by numerical integration. Each group shows the steady state behavior for the eccentricity ratio ε (either left or right), the deflection D, and the transmitted force F_t, each versus the rotation speed Ω^*.

It is evident from Figure 5, which illustrates the behavior of the uncavitated model, that the presented algorithm gives very close results to those obtained by numerical integration. Also, an agreement between the two methods is observed in Figure 6 which shows the behavior of the cavitated model, regardless of the higher values appearing in group (a) which represent other steady states (El-Shafei, 1990, 1991). These additional steady states in the nonlinear model appear in regions of multiple solution and are due to the nonlinearity. They are difficult to obtain by numerical integration since they require tedious trial and error (Taylor and Kumar, 1980)

It should be noted that only the odd modes appear in Figures 5 and 6, since, due to the symmetry of the rotor, the even modes have nodes at the location of the exciting force as shown in Figure 4, and thus are not excited.

To demonstrate the facilities of the suggested algorithm, further program runs are performed on distinct cases, by changing the system parameters for example for different values of the unbalance. Figures 7 and 8 illustrate the effect of increasing the value of the unbalance g^* considering both models. Higher unbalance values increase the possibility of the appearance of nonlinear phenomena such as jump resonance, that is, the rotor would exhibit a jump from a certain whirling orbit to another at same frequency, which is obvious in Figure 8.

As discussed in the previous paragraph, it is possible to study the effect of the different parameters such as the unbalance value g and the bearing parameter B. Also, it is possible to investigate the effect of the bearing and the support stiffness on the behavior of the rotor-bearing assembly through critical speed analyses. It is not possible to achieve this facility by numerical integration, since the execution time needed for one program run would be extremely huge, which emphasizes the algorithm's capabilities. In addition, this algorithm can be used for the optimum design of SFDs, and it is planned to develop the optimum design algorithm in the future.

DISCUSSION

Several important points should be highlighted to emphasize the contributions made by this paper:

1. Squeeze Film Dampers are nonlinear devices. Modal analysis is a linear process. One major contribution of this paper is the use of modal analysis for a nonlinear device, i.e. using modal analysis for a nonlinear system is generally novel.
2. Gyroscopic effects are included in the model through the critical speed analysis to obtain the planar modes. For planar modes, which by definition assume similarity in the x and y directions and imply circular orbits, one does not need to include the Gyroscopic effects in the modal analysis, since left and right eigenvectors are not obtained (see Gunter et al., 1978). However, the gyroscopic effects were included in the Transfer Matrix program used to obtain the critical speeds.
3. Regarding the speed of the proposed algorithm, the iterative algorithm developed by Greenhill and Nelson (1981) was tested by El-Shafei and Eranki (1994) and later by Bayoumi (1995), using a Finite Element program. For each point on

the unbalance response curve the iterative algorithm of Greenhill and Nelson (1981) took about 1 minute for each point when implemented on the same 486 computer, and the speed of execution will depend on the complexity of the rotor system (Bayoumi, 1995). The power and speed of the proposed algorithm in this paper, and the benefit of using a polynomial in Ω, is that the full unbalance response curve (about 300 points) is obtained in 13 minutes, independent of the complexity of the rotor. So in comparison to the steady state algorithm of Greenhill and Nelson to obtain the full unbalance response one is comparing 5 hours (300 points x 1 minute) versus 13 minutes! This is quite a tremendous computer saving that the proposed algorithm provides since:

a) The Finite Element program is not used on line, but rather the proposed algorithm can be considered as post-processing for the results of either the Finite Element or Transfer Matrix, which are only used to obtain the planar modes.
b) Modal analysis is used as a basis for algorithm development, thus the algorithm is independent of the complexity of the rotor system.
c) The power of the algorithm of a polynomial in frequency is fully exploited to obtain the full unbalance response.

The result is an elegant algorithm relying on the previous work of Gunter et al. (1978), Taylor and Kumar (1980) and El-Shafei (1990) to obtain an extremely fast algorithm to obtain the full nonlinear unbalance response of a multi-mode rotor on Squeeze Film Dampers. In comparison, the work of Mclean and Hahn (1983) did not use modal analysis, but rather developed an algorithm that exploits the characteristics of a circular orbit to obtain the response of a multi-mode rotor on squeeze film dampers, however their technique needs to be developed mathematically for each particular rotor, and the mathematics can be cumbersome for a complicated rotor, while our algorithm does not depend on the rotor configuration, rather all what is needed are the rotor modes.

CONCLUSION

A fast algorithm to obtain the steady state unbalance response for a multiple-mode rotor incorporating short squeeze film dampers is developed based on planar modal analysis theory. The modal analysis is implemented on the linear part of the rotor equations, since SFDs add nonlinearities to the model. Undamped critical speed analysis is done to obtain the rotor eigenvalues and eigenvectors. The rotor is assumed to exhibit a centered circular whirl, thus the system differential equations are reduced to nonlinear algebraic ones. Further algebraic manipulations are done to obtain a polynomial in the rotor rotation speed with the purpose of obtaining full unbalance response directly avoiding tedious trial and error and false convergence. The developed algorithm is applied to a conventional rotor to obtain its unbalance response. Results are compared to those obtained from numerical integration of the system differential equations. The comparison, as applied to both uncavitated and cavitated models, showed that both methods agreed well together. The introduced technique proved its robustness and efficiency in saving execution time, which is extremely dramatic in comparison to the numerical integration. In addition, it has the facility of obtaining all possible solutions. This fast algorithm allows parametric studies to be performed and can be used in the optimum design of SFDs.

REFERENCES

Bayoumi, H. N., 1995, "Development of a Finite Element Program for Nonlinear Rotordynamics analysis Using Equivalent Linearization", M.Sc. Thesis, Cairo University.

Bonneau, O., Kassai, A., Frene, J., and Der Hagopian, J., 1989, "Dynamical Behavior of an Elastic Rotor with Squeeze Film Damper" Eurotrib 89, Helsinki, Finland, Proceedings Vol. 4, pp145-149.

Cooper, S., 1963, "Preliminary Investigation of Oil Films for the Control of Vibration", Lubrication and Wear Convention, I. Mech. E., pp. 305-315.

El-Shafei, A., 1990, "Unbalance Response of a Jeffcott Rotor Incorporating Short Squeeze Film Dampers", Journal of Engineering for Gas Turbine and Power, Trans. ASME, Vol. 112, No.4, pp. 445-453.

El-Shafei, A., 1991, "Unbalance Response of Jeffcott Rotor Incorporating Long Squeeze Film Dampers", Journal of Vibration and Acoustics, Trans. ASME, Vol. 113, No.1, pp. 85-94.

El-Shafei, A. And Eranki, R. V., 1994, "Dynamic Analysis of Squeeze Film Damper Supported Rotors Using Equivalent Linearization", Journal of Engineering for Gas Turbine and Power, Trans. ASME, Vol. 116, No. 3, pp. 682-691.

Freidland, B., 1986, "Control System Design (An Introduction to State-Space Theory)", McGraw-Hill, Inc., pp. 88-99

Greenhill, L., and Nelson, H. D., 1981 "Iterative Determination of Squeeze Film Damper Eccentricity for Flexible Rotor Systems", ASME Paper 81-DET-87.

Gunter, E.J., Choy, K.C., and Allaire, P.E., 1978, "Modal Analysis of Turborotors Using Planar Modes-Theory", Journal of the Franklin Institute, Vol. 305, No. 4, pp. 221-243.

Hathout, J.P., El-Shafei, A., and Youssef, R., 1995, "Active Control of Multi-Mode Rotor-Bearing System Using HSFDs", presented at the Tribology Conference, Orlando, FL., October, accepted for publication in the Journal of Tribology, Trans. ASME

IMSL MAT/LIBRARY-FORTRAN subroutines for Mathematical Applications, Version 1.0, April 1987.

Meirovitch, L., 1986, "Elements of Vibration Analysis", McGraw-Hill.

Mclean, L. J., and Hahn, E. J., 1983, "Unbalance Behavior of Squeeze Film Damped Multi-Mass Flexible Rotor Bearing Systems", ASME Journal of Lubrication Technology, Vol. 105, 1, pp. 22-28.

Mohan, S., and Hahn, E. J., 1974, "Design of Squeeze Film Damper Supports for Rigid Rotors", ASME Journal of Engineering for Industry, Vol. 96, pp. 976-982.

Taylor, D. L., and Kumar, B. R. K., 1980, "Nonlinear Response of Short Squeeze Film Dampers", ASME Journal of Lubrication Technology, Vol. 102, pp. 51-58.

Taylor, D. L., and Kumar, B. R. K., 1983, "Closed Form Steady State Solution for the Unbalance Response of a Rigid Rotor in Squeeze Film Damper", ASME Journal of Engineering for Power, Vol. 105, No. 3, pp. 551-559.

White, D.C., 1972, "The Dynamics of a Rigid Rotor Supported on Squeeze Film Dampers", Conference on Vibrations of Rotating Machinery, Proc. I. Mech. E., pp. 213-229.

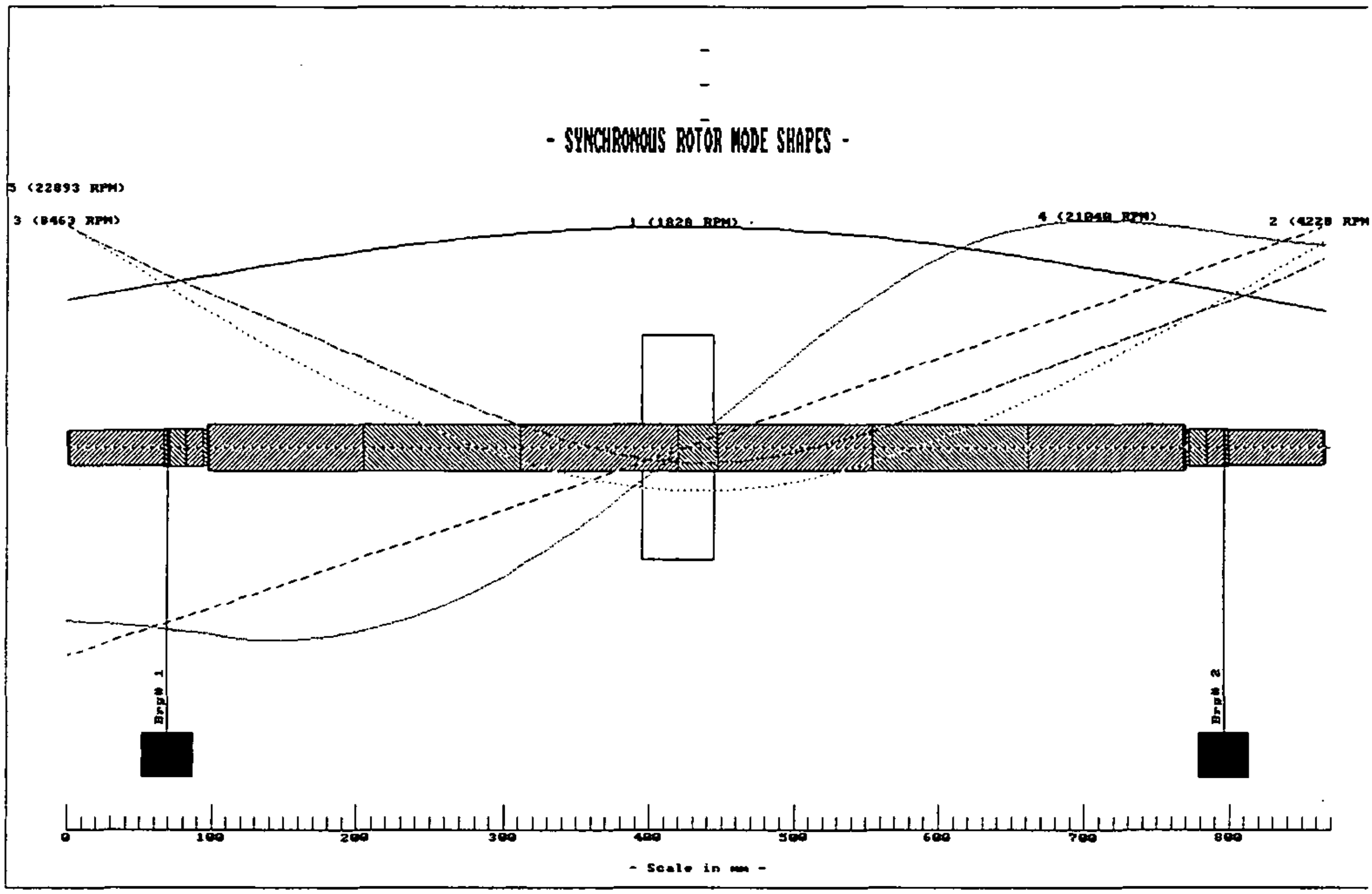

Figure 4 The Studied rotor and its mode shapes

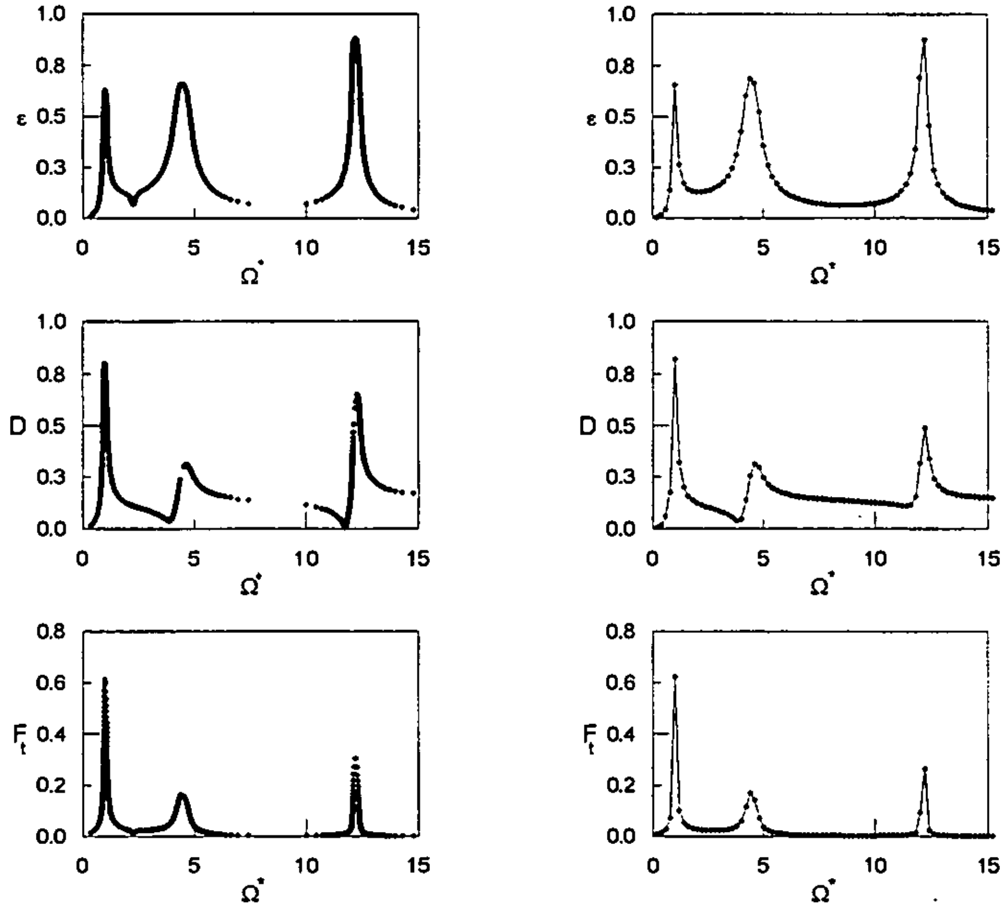

Group (a) Proposed technique

Group (b) Numerical integration method

Figure 5 Unbalance response of the uncavitated model, g = .1

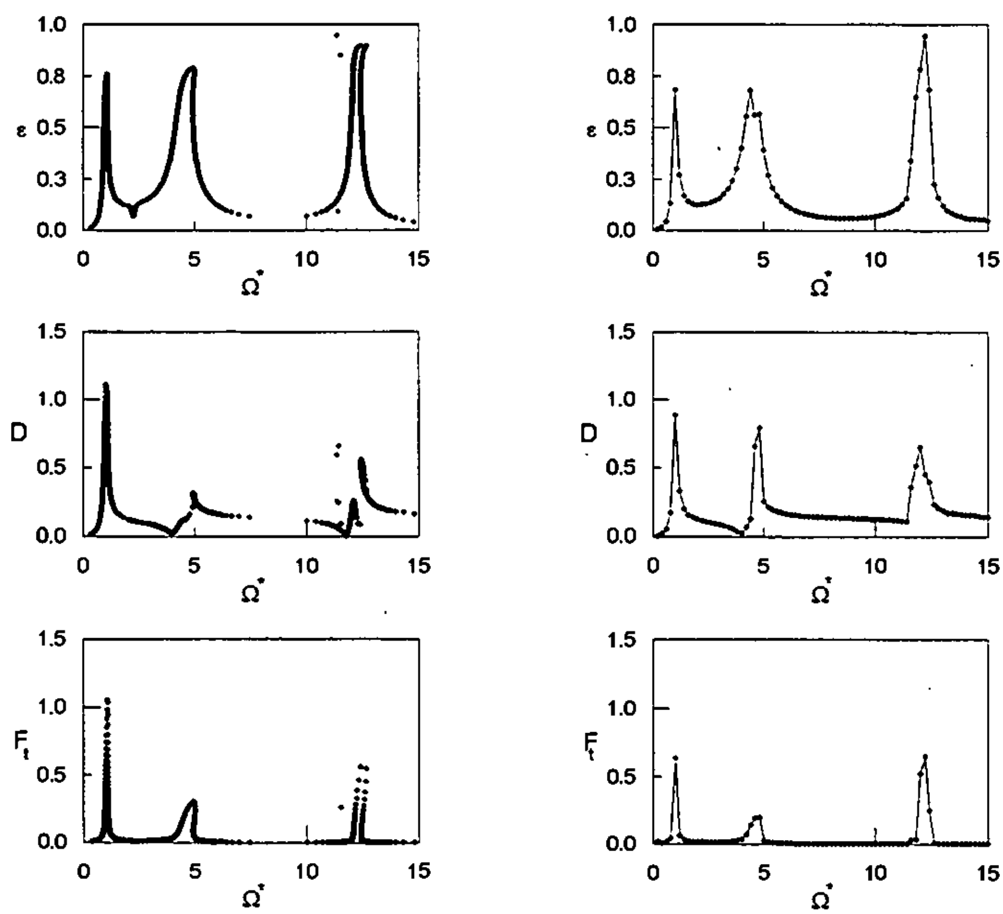

Group (a) Proposed technique

Group (b) Numerical integration method

Figure 6 Unbalance response of the cavitated model, g = .1

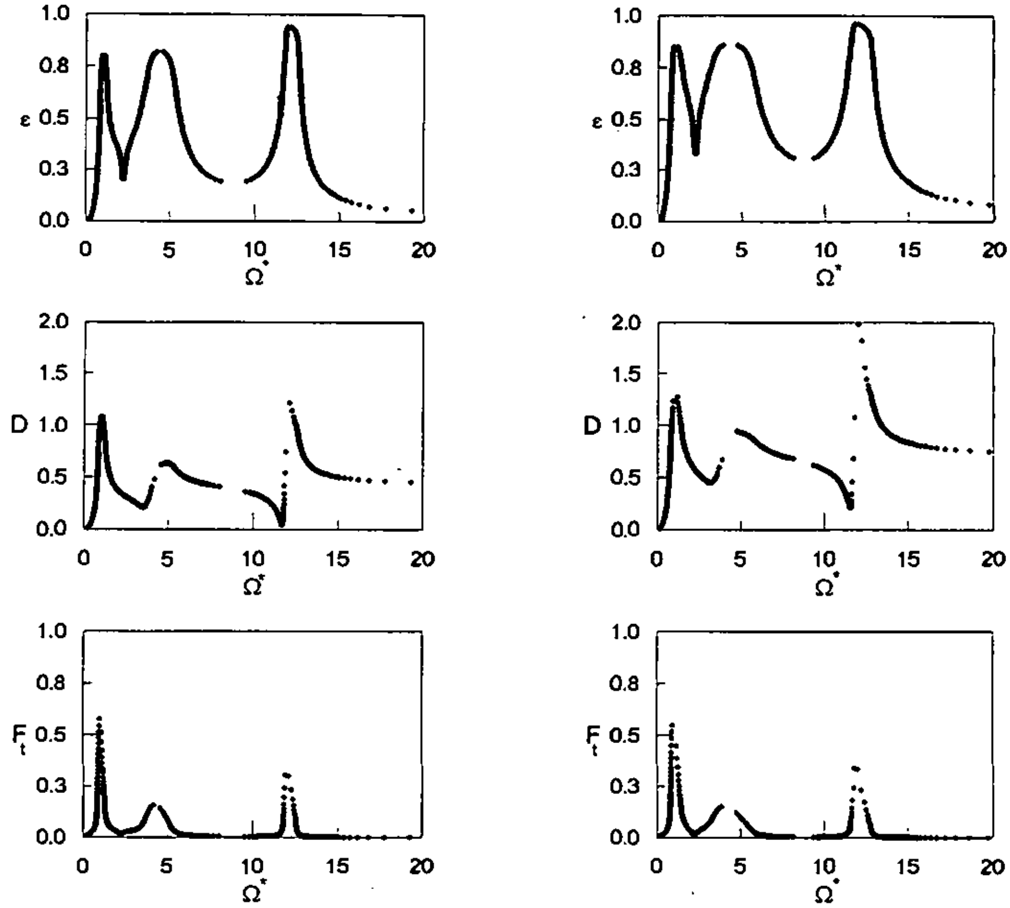

Group (a) g = .3

Group (b) g = .5

Figure 7 Unbalance response of the uncavitated model

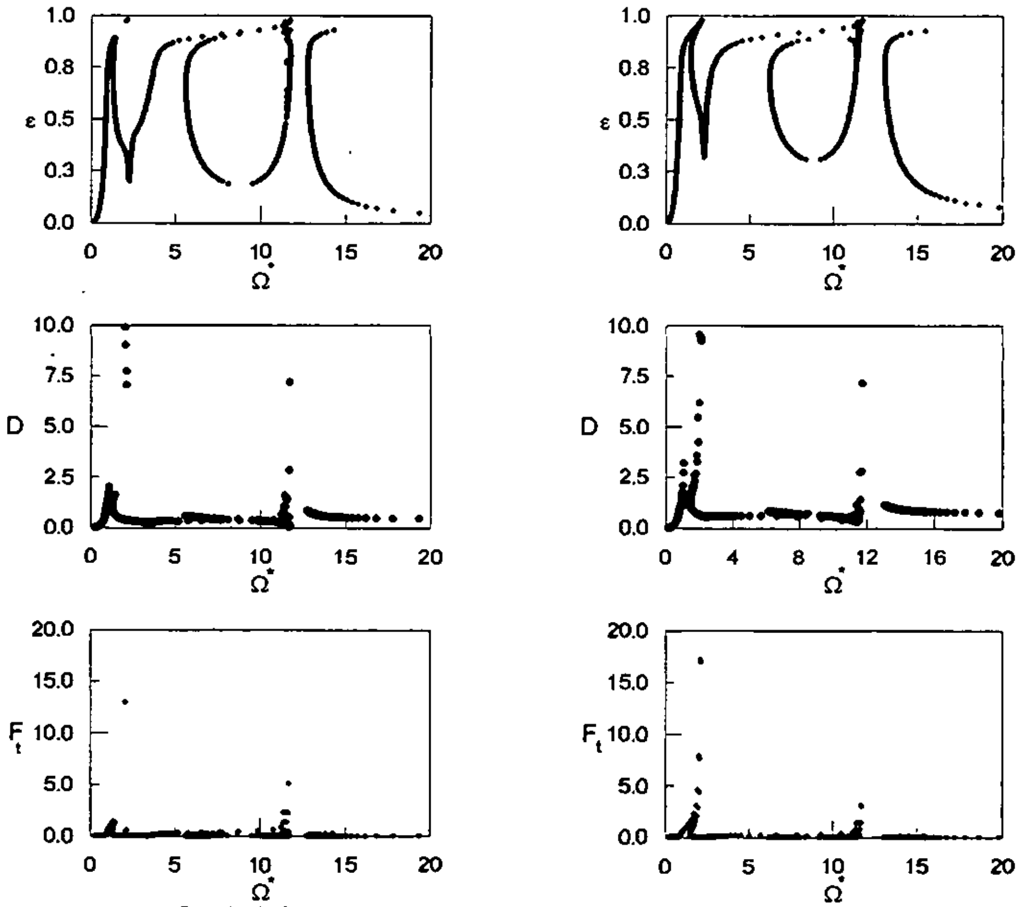

Group (a) g = .3

Group (b) g = .5

Figure 8 Unbalance response of the cavitated model